Fitness in chronic heart failure : effects of exercise training and of biventricular pacing

Gademan, M.

Hedde van de Vooren[1]
Maaike G.J. Gademan[1]
Cees A. Swenne[1]
Ben J. TenVoorde[2]
Martin J. Schalij[1]
Ernst E. van der Wall[1]

[1]*Department of Cardiology, Leiden University Medical Center, Leiden, The Netherlands*
[2]*Department of Physics and Medical Technology, Vrije Universiteit Medical Center, Amsterdam, the Netherlands*

CHAPTER 3

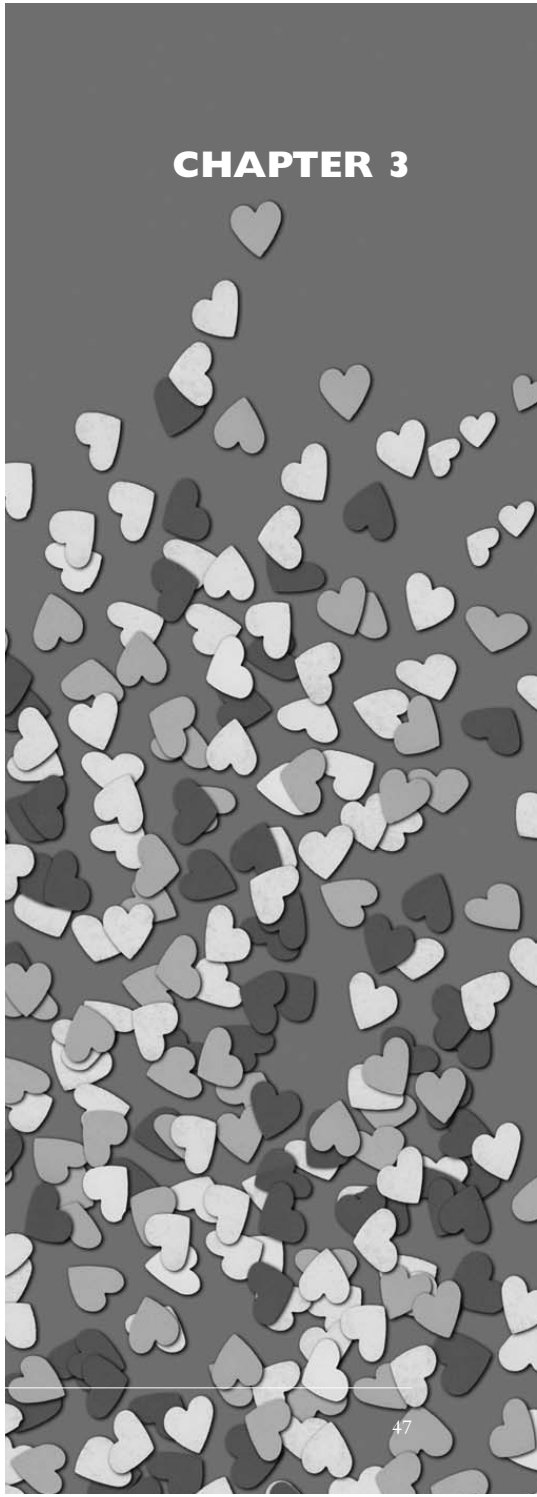

BAROREFLEX SENSITIVITY, BLOOD PRESSURE BUFFERING AND RESONANCE: WHAT ARE THE LINKS? COMPUTER SIMULATION OF HEALTHY SUBJECTS AND HEART FAILURE PATIENTS

J Appl Physiol 2007;102:1348–1356

ABSTRACT

Objectives. The arterial baroreflex buffers slow (< 0.05 Hz) blood pressure (BP) fluctuations, mainly by controlling peripheral resistance. Baroreflex sensitivity (BRS), an important characteristic of baroreflex control, is often noninvasively assessed by relating heart rate (HR) fluctuations to BP fluctuations; more specifically, spectral BRS assessment techniques focus on the BP to HR transfer function around 0.1 Hz. Scepsis about the relevance of BRS to characterize baroreflex-mediated BP buffering is based on two considerations: 1) baroreflex modulated peripheral vasomotor function is not necessarily related to baroreflex-HR transfer, and 2) though BP fluctuations around 0.1 Hz (Mayer waves) might be related to baroreflex blood pressure buffering, they are merely a not-intended side-effect of a closed loop control system.

Methods. To further investigate the relationship between BRS and baroreflex-mediated BP buffering, we set up a computer model of baroreflex BP control to simulate normal subjects and heart failure patients. Output variables for various randomly chosen combinations of feedback gains in the baroreflex arms were BP resonance, BP buffering capacity and BRS.

Results. BP buffering and BP resonance are related expressions of baroreflex BP control and depend strongly on the gain to the peripheral resistance. BRS is almost uniquely determined by the vagal baroreflex gain to the sinus node.

Conclusions. BP buffering and BRS are unrelated unless coupled gains in all baroreflex limbs are assumed. Hence, the clinical benefit of a high BRS is most likely to be attributed to vagal effects on the heart instead of to effective blood pressure buffering.

INTRODUCTION

In daily life, multiple processes perturb blood pressure. The duration of these challenges varies widely. For example, respiration makes blood pressure fluctuate with every breath[13] while physical or mental stress elevate blood pressure for minutes or even longer. The arterial baroreflex is a negative feedback mechanism that effectively buffers such incidental blood pressure fluctuations[11,20,21,23]. In negative feedback systems, feedback delay often causes resonance in a given frequency band; this is the price to be paid for effective buffering at other frequencies. Resonance in blood pressures[5,8,12,31,49] manifests in the form of the well known Mayer[22,33] waves (beat-to-beat blood pressure oscillations with a frequency around 0.1 Hz / periodicity around 10 s). Effective baroreflex blood pressure buffering occurs below the Mayer frequency[10,16].

Besides a sympathetic limb that modulates peripheral resistance, the baroreflex has also sympathetic and parasympathetic (vagal) limbs that influence cardiac contractility, venous return and cardiac rhythm. Usually, baroreflex functioning is characterized by baroreflex sensitivity (BRS). This index of baroreflex vigor is defined as the reflex-induced change in interbeat interval in ms per mmHg blood pressure change[14,34,36,44]. The prognostic value of BRS, and the favorable consequences of successful interventions with BRS, has amply been demonstrated[27,28].

Little is known, however, about the representativeness of this index for the efficacy of blood pressure buffering. There are two reasons to be skeptical in this respect:

1) By definition — interbeat interval change per unit blood pressure change — BRS is bound to characterize baroreflex mediated effects on the heart, while the baroreflex buffers blood pressure mainly by controlling peripheral resistance[2,30]
2) Oftentimes being assessed in the Mayer frequency range of spontaneous heart rate and blood pressure fluctuations[15,39], BRS might represent resonance- rather than buffering baroreflex characteristics.

We addressed these skepticisms by simulations with a hybrid mathematical model of baroreflex blood pressure and heart rate control, composed of hemodynamic elements that are evaluated on a beat to beat basis, linked to a time-continuous modeled neural control part. By changing some parameter settings the model mimics physiological as well as pathological hemodynamic and autonomic conditions.

By simulating with various gain combination values, we quantified the role of the sympathetic and parasympathetic gains in the three baroreflex limbs for blood pressure variability (BPV) and heart rate variability (HRV) under physiologic and pathologic conditions. From the obtained systolic blood pressure and interbeat interval values, relations between BRS and blood pressure buffering, and between blood pressure buffering and resonance were examined.

METHODS

The simulation model we used for this study represents short-term human blood pressure control without breathing modulation. It is tuned for supine posture. This model — programmed in Matlab Simulink (*The MathWorks, Inc., Natick*, MA) — is, apart from some modifications, similar to the model as earlier designed and validated by TenVoorde and Kingma[46].

Model description

A gross overview of the autonomically controlled model is given in *Figure 1* (see *Table 1* and *Table 2* for abbreviations and model parameters). The model represents the systemic circulation and consists of three sections: a hemodynamic section, a baroreceptor section and an autonomic control section. The model generates output in the form of time dependent systolic blood pressure values (SBP, mmHg) and interbeat interval values (IBI, ms) by using a sinusoidal pressure probe (frequency adjustable, amplitude fixed at 1 mmHg) as an input signal. This apparently small perturbation at the input of the baroreflex produces reduced SBP fluctuations (amplitude <1 mmHg,

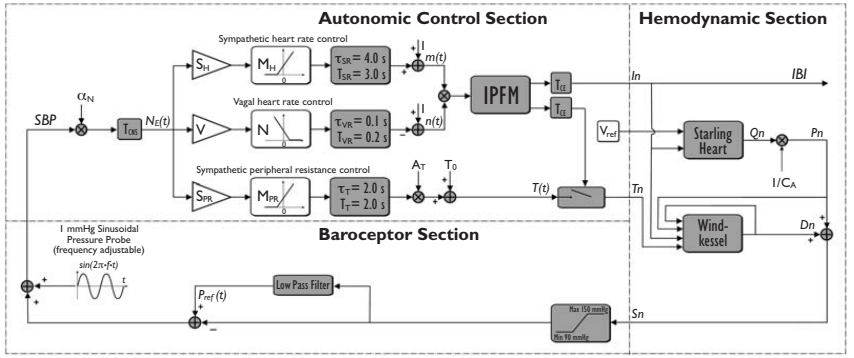

Figure 1. *Model of baroreflex arterial blood pressure control. The model variables and model parameters are described in Table 1 and Table 2. Model sections and parameters are discussed in the Methods section. Note that variables (i.e., continuous signals and sample and hold signals) are denoted italic. Adjustable parameters (denoted bold) are placed in white boxes, fixed model divisions are placed in grey boxes.*

buffering) but also Mayer waves (amplitude >1 mmHg, resonance), depending on the frequency of the pressure probe.

Hemodynamic section

In the hemodynamic section, all signals are sample-and-hold signals: the beat-to-beat varying cardiovascular signals are modeled in elementary difference equations. All values are adapted when a new heartbeat emerges. Stroke volume Q_n is produced by the one-chamber Starling heart. It depends on interbeat interval I_n, venous return volume V_n and a contractility volume term C_n:
$Q_n = \delta_n \cdot V_n + C_n$,
where δ_n is a left ventricle filling factor:
$\delta_n = 0.5 + 0.5\, I_n / 1000$.
As this model will only be used to simulate different autonomic control states, rather than different hemodynamic states (like standing posture), changes in cardiac contractility and venous return appear to generate only very small fluctuations in stroke volume (<5%). Therefore, we simplified above relation into:
$Q_n = \delta_n \cdot V_{ref}$,
where Starling heart filling parameter V_{ref} indicates the stroke volume when $\delta_n = 1$.
Stroke volume, Q_n, assuming a constant arterial compliance C_A, determines pulse pressure P_n by: $P_n = Q_n / C_A$.
A systemic Windkessel simulates diastolic blood pressure D_n:

$$D_n = \left(D_{n-1} + \frac{1}{2}P_{n-1}\right)e^{-\frac{I_n}{T_n}}.$$

The Windkessel time constants T_n is controlled by the baroreflex (see autonomic control section), and is directly associated with total peripheral resistance. Although it is usual to compute diastolic pressure as the exponential decay of systolic pressure, we used this slightly modified formula to obtain more accurate systolic blood pressure values. Finally, systolic pressure S_n is computed by adding P_n and D_n.

Table 1. *Model parameters and values under physiological (phys.) and pathological (path.) conditions.*

Symbol	Description	Value
A_T	Sympathetic peripheral resistance control sensitivity coefficient	11500 ms/nu
α_N	Baroreceptor sensitivity coefficient	0.004 nu/mmHg
f	Pressure probe frequency	0.0033 – 0.3 Hz
M_H	Sympathetic tone to the heart	1.2 (phys.) / 1.5 (path.)
M_{PR}	Sympathetic tone to the peripheral vasculature	1.2 (phys.) / 1.25 (path.)
N	Vagal tone to the heart	0.5 (phys.) / 0.6 (path.)
R_0	Intrinsic heart rate	100 beats/min [25]
S_H	Sympathetic baroreflex gain to the heart multiplier	0.0 – 3.0
S_{PR}	Sympathetic baroreflex gain to the peripheral resistance multiplier	0.0 – 3.0
T_0	Sympathetic peripheral resistance control intrinsic value	1800 ms
T_{SR}	Sympathetic heart rate control time delay	3000 ms [48]
t_{SR}	Sympathetic heart rate control time constant	4000 ms [48]
T_T	Sympathetic peripheral resistance control time delay	2000 ms
τ_T	Sympathetic peripheral resistance control time constant	2000 ms
T_{VR}	Vagal heart rate control time delay	200 ms [35]
τ_{VR}	Vagal heart rate control time constant	100 ms [4,26]
T_{CE}	Delay of cardiac event from SA-trigger to pressure rise	250 ms
T_{CNS}	Delay in central nervous system processing	100 ms [24]
V	Vagal baroreflex gain multiplier	0.0 – 3.0
V_{ref}	Stroke volume at 1000 ms filling time	80 ml (phys.) / 60 ml (path.)

Baroreceptor section

The baroreceptors are modeled linearly within a range of threshold of 90 mmHg and saturation level of 150 mmHg. At the baroreceptors, the systolic blood pressure S_n is compared with a low-pass filtered systolic blood pressure reference value. This value functions as a dynamic blood pressure set point, mimicking the physiologic process of baroreceptor resetting[47,50,51]. The pressure variability source is added at the input of the baroreflex, rendering a sample and hold systolic blood pressure variability signal SBP, the first model output signal.

Autonomic control section

In the time-continuous autonomic control section, SBP is converted into an afferent neural signal N_E by factorizing this signal by the baroreceptor sensitivity coefficient α_N. This signal concerns as input for three effectors:
- vagal heart rate control (output: vagal signal *n*);
- sympathetic heart rate control (output: sympathetic signal *m*);
- sympathetic peripheral resistance control (output Windkessel time constant *T*);

The vagal signal *n* represents vagal heart rate deceleration ($0<n<1$), while the sympathetic signal *m* represents sympathetic heart rate acceleration ($m>1$).

The three effectors are modeled in frequency-dependent functional blocks, with specific sensitivity coefficients, time constants, time delays and by autonomic tones (N, M_H and M_{PR}; see *Table 1* for actual values). In addition to these model parameters, extra baroreflex gain multipliers (S_H, V and S_{PR}) were added to strengthen or weaken the role of each baroreflex effector.

The neural time-continuous part and the hemodynamic beat-to-beat part are interconnected by an Integral Pulse Frequency Modulator (IPFM), which simulates cardiac pacemaker function[18]. Rosenblueth and Simeone[40] have demonstrated that combined sympathetic and vagal influences on the sinus node contribute to the actual heart rate *R* according to the following relationship: $R = R_0 \cdot m \cdot n$, where R_0 is the intrinsic heart rate. Integration of incoming neural activity results in the generation of the heart interval length I_n[18]. This interbeat interval IBI is the second model output signal.

Adjustable model parameters

Thus, the model is controlled by seven parameters: one (V_{ref}) for stroke volume, three (M_H, N and M_{PR}) for autonomic outflow, and three (S_H, V and S_{PR}) multipliers for the gains in the three baroreflex limbs.

The first four parameters for stroke volume and autonomic outflow were set as two fixed

Table 2. *Model variables: sample and hold (n) or time dependent (t). bpm: beats per minute*

Symbol	Description	Unit
Dn	Diastolic blood pressure	mmHg
δn	Left ventricle filling factor	-
I_n, IBI	Interbeat interval	ms
$m(t)$	Sympathetic heart rate acceleration signal	-
$n(t)$	Vagal heart rate deceleration signal	-
$N_E(t)$	Neural error driving signal	nu
P_n	Pulse pressure	mmHg
$P_{ref}(t)$	Reference systolic blood pressure	mmHg
Q_n	Stroke volume	ml
$R(t)$	Heart rate	bpm
S_n, SBP	Systolic blood pressure	mmHg
t	Simulation time	s
T_n, $T(t)$	Windkessel time constant	ms
Vn	Venous return (expressed in blood volume units)	ml

combinations (*Table 1*) to represent either normal physiological, or abnormal pathological resting conditions. With an increased sympathetic tone to the heart and to the peripheral resistance, and decreased parasympathetic tone and reference stroke volume, the pathological parameter settings represent a serious pathologic condition resembling congestive heart failure. Compared to the physiological conditions, the resting heart rate is higher (90 bpm instead of 60 bpm), and the average systolic blood pressure is slightly lower (114 mmHg instead of 120 mmHg).

The last three parameters serve as potentiometers (multipliers) on the vagal and sympathetic baroreflex gains to the heart and to the peripheral resistance;
$V = S_H = S_{PR} = 1$ is the reference value that is to represent a normally working baroreflex.

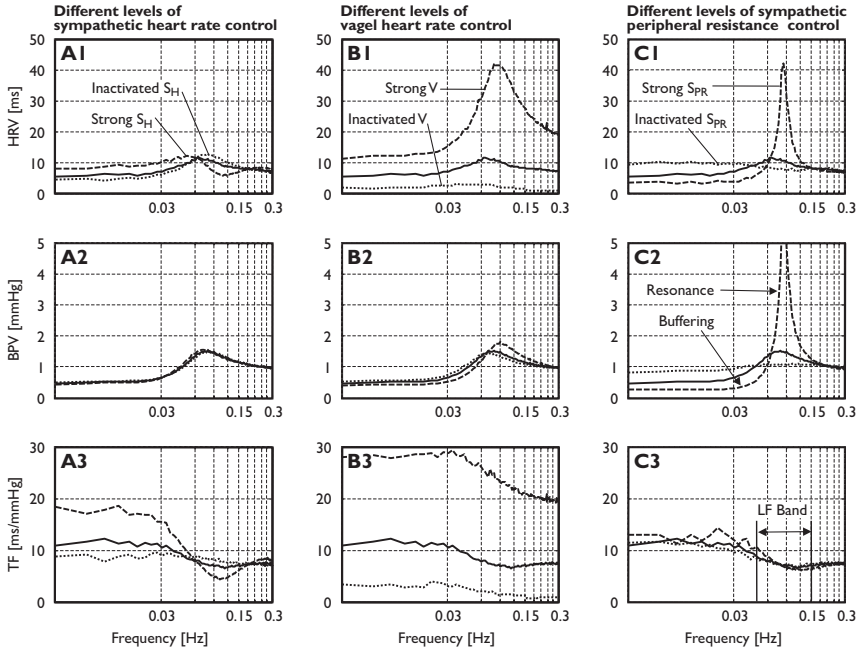

Figure 2. *Examples of simulated heart rate variability (HRV; A1, B1, C1), blood pressure variability (BPV; A2, B2, C2) and transfer function (TF; A3, B3, C3) frequency characteristics. Note that frequency axes are log scaled. For these simulations, the model parameters for stroke volume and autonomic outflow, $-V_{ref}$, M_H, M_{PR} and N–, were kept fixed at physiological values (see Table 1). The baroreflex gain multipliers S_H, V and S_{PR} were varied around $S_H/V/S_{PR}$ = 1/1/1 (solid line in all panels) in the following way:*
Panels A: dotted line: $S_H/V/S_{PR}$ = 0/1/1 (inactivated S_H), dashed line: $S_H/V/S_{PR}$ = 3/1/1 (strong SH);
Panels B: dotted line: $S_H/V/S_{PR}$ = 1/0/1 (inactivated V), dashed line: $S_H/V/S_{PR}$ = 1/3/1 (strong V);
Panels C: dotted line: $S_H/V/S_{PR}$ = 1/1/0 (inactivated SPR), dashed line: $S_H/V/S_{PR}$ = 1/1/3 (strong SPR).
BPV and HRV amplitudes have to be related to the driving force of the sinusoidal pressure probe (1 mmHg).
BPV = blood pressure variability (amplitude of SBP fluctuations); HRV = heart rate variability (amplitude of IBI fluctuations); TF = modulus of the SBP-to-IBI transfer function.

When one of these parameter values equals 0, the corresponding limb of the baroreflex does not react to changes of SBP with respect to the reference value and the corresponding effector output becomes the (fixed) tone. A value of 0.5 corresponds to weak involvement. The maximum value of these parameters is 3; this value corresponds to a strong involvement of a given baroreflex limb, e.g., as found in highly trained subjects.

Simulations and frequency characteristics

For a given combination of the seven model parameter values, 100 simulation runs were done. A single simulation run served to determine one SBP variability (BPV) frequency component, one IBI variability (HRV) frequency component and the modulus of the SBP-TO-IBI transfer function (TF, necessary to compute BRS) frequency component, at a given frequency of the sinusoid pressure probe. A single simulation run was executed as follows. First, the model was run till steady state conditions were met. Then, cubic splines were fitted through the resulting output signals to obtain the amplitudes of the SBP- and IBI fluctuations, caused by the pressure probe. Finally, the corresponding TF frequency component was computed by dividing HRV (the amplitude of the IBI fluctuations) by BPV (the amplitude of the SBP fluctuations). The 100 simulation runs were done to construct the complete frequency characteristics of BPV, HRV and TF by computing all frequency components between 0.003 Hz and 0.300 Hz (step 0.003 Hz).

A total of 162 frequency characteristics of HRV, BPV and TF were made for both the physiological as well as for the pathophysiological conditions. These 162 frequency characteristics were made to represent 162 different combinations of baroreflex gain multiplier settings. One-hundred fifty gain multiplier combinations were randomly chosen to simulate uncoupled baroreflex gains (values between 0 and 3 from uniform distributions for V, S_H and S_{PR}). In addition, 12 other $V/S_H/S_{PR}$ combinations were made to simulate coupled baroreflex gains (0.5/0.5/0.5, 1/1/1, 1.5/1.5/1.5, 2/2/2, 2.5/2.5/2.5, 3/3/3). Besides these multiplier combinations, an extra set of simulation results (obtained with $V/S_H/S_{PR}$ combinations 0/1/1, 3/1/1, 1/0/1, 1/3/1, 1/1/0, 1/1/3) was made for the generation of *Figure 2*.

Main derived simulation variables: BRS, SBP buffering capacity, SBP resonance

After having computed a full BPV, HRV and TF characteristic, we determined the following variables. BRS was computed as the averaged magnitude of TF in the low-frequency (LF, 0.05–0.15 Hz)[15,37,39]. This band incorporates the Mayer frequencies. SBP *buffering capacity* was expressed as the amplitude of the original perturbation (the 1 mmHg sinusoidal pressure probe) divided by the BPV amplitude at the lowest simulated frequency component (0.0033 Hz, which is still well above the baroreceptor resetting frequency[47]). E.g., when the BPV at the lowest frequency component had an amplitude of 0.25 mmHg, the buffering capacity was 4. Maximal SBP *resonance* (in the LF band) was expressed as the maximal BPV divided by the amplitude of the original perturbation. To determine the relative importance of V, S_H and S_{PR} for BRS and blood pressure buffering/resonance, multiple linear regressions were done. For these regressions, only the simulations made with random generated baroreflex gain multipliers were used.

RESULTS

The simulation results obtained under physiological and pathological conditions (see Table 1) differ quantitatively (more outspoken characteristics under physiological conditions) rather than qualitatively: all frequency characteristics are smooth, and buffering occurs at the lowest frequencies while resonance occurs at the Mayer frequency around 0.1 Hz. *Figure 2* displays examples of some HRV-, BPV- and TF

frequency characteristics obtained under physiological conditions. This Figure consists of three sets of HRV, BPV and TF frequency characteristics, in each of which one of the three effectors was weakened or strengthened, i.e., baroreflex gain multipliers, V, S_H, or S_{PR} was increased to 3 (strong) or reduced to 0 (inactivated) with respect to the default value of 1 (normal), while the other two baroreflex gain multipliers were kept at their default values of 1 (normal).

Panel A3 shows an unexpected influence of sympathetic heart rate control on IBI: the transfer function in the LF band (i.e. BRS) even decreases when control is strengthened (strong S_H). Obviously, blood pressure buffering and resonance are completely insensitive for changes in the sympathetic gain to the heart (panel A2).

Panels B1-B3 show how the HRV, BPV and TF frequency characteristics react when the

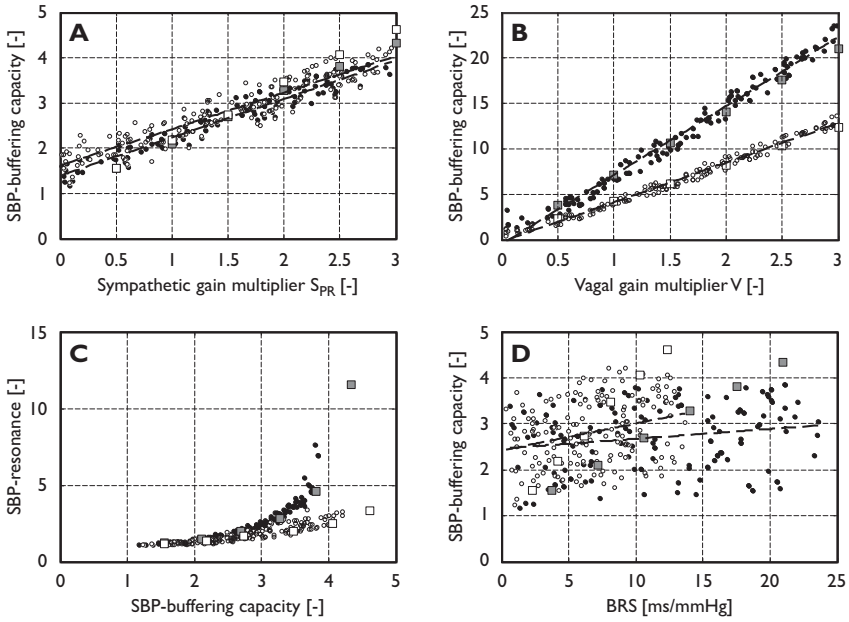

Figure 3. *Main graphical representations of the simulation results. Panel A: systolic blood pressure (SBP) buffering capacity increases with increasing sympathetic baroreflex gain to the peripheral resistance. Panel B: baroreflex sensitivity (BRS) increases with increasing vagal baroreflex gain to the heart. Panel C: SBP resonance increases with increasing SBP buffering capacity. Panel D: SBP buffering capacity is only weakly related to baroreflex sensitivity. Filled circles and squares: physiological conditions; open circles and squares: pathological conditions. Circles (small): simulations with uncoupled (random generated) baroreflex gain multiplier combinations; squares (larger): simulations with coupled baroreflex gain multiplier combinations: $S_H/V/S_{PR}$ = 0.5/0.5/0.5, 1/1/1, 1.5/1.5/1.5, 2/2/2, 2.5/2.5/2.5, 3/3/3. Dashed lines: linear regressions in the random data (hence, scouting simulations with coupled baroflex gain multiplier combinations excluded). See text for further explanation.*

vagal heart rate control is weakened or strengthened (multiplier V assumes the value 0 or 3 respectively, multipliers S_H and S_{PR} are kept at a value of 1). Here, the impression arises that multiplier V strongly influences HRV and the BRS, while it does not affect the resonance and buffering behavior (relatively little differences in resonance and buffering are seen in panel B2).

Panels C1-C2 show the striking effect of a strengthened sympathetic peripheral resistance control (multiplier S_{PR} assumes the value of 3, multipliers V and S_H are kept at a value of 1) on the HRV and BPV frequency characteristics. Panel C2 shows that the original sinusoidal disturbance of SBP by the 1 mmHg pressure probe (see *Figure 1*) is strongly weakened (buffered) for the lowest frequencies, is amplified (resonance) over nearly the whole LF band, and returns to about 1 mmHg for higher frequencies. Larger part of this effect — especially the resonance phenomenon — disappears under normal control (multiplier S_{PR} assumes the value of 1). The frequency characteristic is almost flat when control is absent (multiplier S_{PR} assumes the value of 0). The shapes of the HRV frequency characteristics in panel C1 grossly follow the BPV characteristics. As expected, the TF frequency characteristics (panel C3) are very much similar for all three S_{PR} values 0, 1 and 3. In summary, from frequency characteristics C1-C3 the impression arises that sympathetic peripheral resistance control strongly influences resonance and buffering while it does not affect the TF or BRS.

Figure 3 depicts the strongest relations between vagal and sympathetic baroreflex gains, SBP buffering capacity, SBP resonance and BRS, based on the results of multiple linear regression analysis. It pointed out that in a physiological setting 83% of the variance in SBP buffering was attributable to sympathetic peripheral resistance control (multiplier S_{PR}); under pathological conditions this percentage was 78%. Also, 99% of the variance in BRS was attributable to vagal heart rate control (multiplier V); under pathological conditions this percentage was also 99%.

The scatter plot of the SBP buffering capacity as a function of S_{PR}, together with linear fits for the physiological and the pathological data (*Figure 3*, panel A), shows close to perfect linear relationships. Also, there is little difference between the linear fits for the physiological and the pathological simulation results. Obviously, heart rate control, but also the settings of V_{ref} and M_{PR} were of minor importance for blood pressure buffering.

The scatter plot of BRS as a function of V, together with linear fits for the physiological and the pathological data (*Figure 3*, panel B), shows nearly perfect linear relationships. Here, the physiological fit (slope 6.9 $ms \cdot mmHg^{-1}$) and the pathological fit (slope 4.0 $ms \cdot mmHg^{-1}$) differ considerably: with equal vagal gain multipliers, BRS is much larger in physiological conditions.

Figure 3 panel C shows that SBP buffering capacity and SBP resonance have a convex relationship and that the resonance phenomenon is much more prominent in physiological circumstances compared to pathological conditions. The strong link between buffering and resonance follows directly from regression analysis: also here, multiplier S_{PR} attributes the most to variance in SBP resonance (95% under normal conditions, 91% under pathological conditions).

Figure 3, panel D, finally, shows that BRS was almost unrelated to SBP buffering capacity, unless coupled baroreflex gains (simulation results represented by the open and solid squares) are assumed. The squared correlation coefficients of the linear regressions of SBP buffering capacity on BRS were as low as 0.037 (physiological conditions) and 0.083 (pathologic conditions).

DISCUSSION

We used a mathematical model to investigate the relation between baroreflex sensitivity (BRS, an index of baroreflex vigor) and baroreflex mediated blood pressure buffering capacity. This relation is not straightforward since the involved efferent baroreflex limbs (vagal and sympathetic pathways to the heart, and sympathetic pathways to the peripheral vasculature, respectively) differ. Moreover, baroreflex buffering occurs at lower frequencies than the Mayer frequency band in which BRS is noninvasively assessed and in which blood pressure resonates. Whether or not resonance disturbs the transfer function, thus precluding reliable BRS assessment in the Mayer frequency band is not known. Also it is not clear what the relation is between, on one hand, the 'desired' phenomenon of blood pressure buffering at frequencies lower than the Mayer frequency and, on the other hand, the phenomenon of blood pressure resonance in the Mayer frequency band (nothing more than a byproduct of baroreflex mediated blood pressure control[10]).

Simulations with various combinations of baroreflex gains, under physiologic as well as under pathologic conditions (increased sympathetic tone, decreased vagal tone, reduced cardiac stroke volume) yielded frequency characteristics of the transfer function, of HRV and of BPV, and values of BRS, blood pressure buffering capacity and baroreflex resonance in a wide range of conditions that may be met in real life. All frequency characteristics had a smooth character, and even with striking resonance the transfer function did not show discontinuous or deviant behavior when compared with its value below and above the frequency band of resonance (see *Figure 2*). In the following, the simulation results will be discussed in the order they have been presented in *Figure 3*.

Baroreflex gains and blood pressure buffering capacity

Our results suggest a predominant role for the sympathetic limb to the peripheral vasculature for the blood pressure buffering capacity of the arterial baroreflex (*Figure 3*, panel A). There is almost no difference in buffering capacity between the physiological and the pathological conditions. This result clearly illustrates the fact that efficacy of baroreflex mediated blood pressure control rests on dynamic control of the peripheral resistance. Modulation of heart rate by baroreflex mediated modulation of the vagal and sympathetic tone to the heart is not very relevant for blood pressure control in the frequency range of interest for this study (0.05 to 0.3 Hz).

Obviously, the simulation results may not be interpreted in such a way that baroreflex mediated blood pressure buffering in patients is not different from that in healthy subjects. The sympathetic feedback gain to the peripheral vasculature is the decisive factor here. We speculate that this gain will be lower in patients. Hence, it may have been somewhat unrealistic to extend the simulations in pathological conditions to a similar value of S_{PR} than the simulations in physiological conditions. The consequence of our speculation would be that the blood pressure buffering capacity in patients is smaller than that in healthy subjects.

Baroreflex gains and baroreflex sensitivity

BRS is linear with, and depends almost exclusively on the vagal feedback gain to the heart (*Figure 3*, panel B). The slopes of the linear regressions (6.9 and 4.0 ms·mmHg^{-1} with physiological and pathological conditions, respectively) are merely to be explained on the basis of heart rate differences between these two situations and the way the IPFM[18] reacts to fluctuations in vagal tone. The fact that BRS depends on heart rate has been recognized earlier[1] and proposals have been done to normalize BRS on heart rate, or, alternatively, to express BRS in [bpm·mmHg^{-1}] instead of in [ms·mmHg^{-1}]. Such arithmetic operations would change the linear relationships in *Figure 3* panel B in curved ones, but leave the conclusions unaffected that BRS increases with increasing vagal feedback gain and that the vagal feedback gain almost uniquely determines BRS.

The predominant role of the vagal feedback gain on the BRS[38] can also be formulated in a slightly different way: due to the differences in the time constants of the vagal and the sympathetic branches (in our model 0.1 s and 4.0 s, respectively), greater part of HRV is simply vagal transmission of blood pressure variability to the sinus node. This is easily perceived in panels B and C in *Figure 2* and in accordance with the findings of Cevese et al.[9]. When vagal feedback gain is zero (dotted lines in panels B) there is almost no HRV (panel B1) while there still is appreciable BPV (panel B2). When there is appreciable vagal baroreflex feedback gain (solid and dashed lines in panels B, and all lines in panels C) the HRV frequency characteristics in panels B1 and C1 have the same shape as the BPV frequency characteristics in panels B2 and C2. In the case of overt (sympathetically mediated) blood pressure resonance, where the BPV frequency characteristic has a narrow peak (panel C2), a similar 'monochrome' HRV frequency characteristic is seen in panel C1. Alternatively, when there is no outspoken resonance (panel B2), there is 'broad band' HRV (panel B1).

Blood pressure buffering capacity and Mayer waves

Figure 3 panel C illustrates the principle that a negative feedback control system with feedback delay buffers the controlled variable at certain frequencies at the cost of resonance at other frequencies. The baroreflex blood pressure control system as simulated in this study behaves in a way that is very similar to what was experimentally observed[10]. Blood pressure buffering, a major function of the baroreflex, occurs at frequencies below the Mayer waves (resonance in the LF band, *Figure 2* panel C2). Typically, the arterial baroreflex could dampen blood pressure and heart rate responses to stressors that last several minutes. On one hand, neural control of blood pressure by sympathetically induced vasoconstriction is relatively fast (seconds). On the other hand, baroreceptor resetting[47,50,51] limits the maximal duration during which baroreflex mediated buffering of a stressor may continue. In our simulations the BPV frequency characteristics in panels A2, B2 and C2 show that dampening (reduction of the sinusoidal pressure probe disturbance) is strongest for the lowest frequencies.

Although there still exist some controversy about the origin of the observed spontaneous blood pressure and heart rate variations around 0.1 Hz[32], we assume that this phenomenon is due to the dynamics of the closed-loop vasomotor control (arterial peripheral resistance), in which the time delay of a few seconds plays the major role. Building a baroreflex model with negative feedback control, and with parameters estimated from physiologically known data, results in a model that simply shows such resonance behavior, without the need to postulate centrally driven oscillators or (strong) nonlinearities.

Resonance, the price to be paid for buffering, is likely to be useless in terms of homeostasis. At the same time it may be an innocent phenomenon without any negative impact for the organism[22]. The fact that Mayer waves, useless or not, exist, facilitates spectral BRS assessment in the LF band, by creating an input signal (BPV) for the baroreflex of which the output signal (HRV) can easily be measured. There is no inherent signal analysis problem in measuring BRS by the transfer function around the resonance frequency. However, the 180° phase shift caused by the time lag in the sympathetic efferent baroreflex limb to the heart with respect to the phase shift in the efferent vagal limb, that has a much shorter time lag, may cause the sympathetic and vagal limbs to the heart to counteract in the LF band.

This effect will become prominent with

increased sympathetic gain to the heart (see, e.g., *Figure 2*, Panel A1, dashed line). In this respect, lower TF frequencies would constitute a more realistic BRS estimate, because here vagal and sympathetic feedback to the heart is concordant (Panel A3, dashed line). In general, TF values in the LF band are not too different at higher frequencies; TF values increase for lower frequencies (*Figure 2*, Panels A3, B3, C3).

Baroreflex sensitivity and blood pressure buffering capacity

One of the major reasons to perform this study was the question whether or not there is a relation between the primary function of the baroreflex, *i.e.*, blood pressure buffering, and the generally accepted clinical index for baroreflex vigor, BRS. *Figure 3*, panel D shows that this relation does almost not exist. The correlation coefficients of the regression lines of SBP buffering capacity on BRS are very low, and the data are diffusely distributed.

Indeed, vagal control of heart rate (major cause of the BPV-to-HRV transfer and, hence, major determinant of BRS) and sympathetic modulation of the peripheral vasculature (major cause of peripheral resistance adaptations and, hence, a major determinant of blood pressure buffering) become effective via separate efferent pathways of the baroreflex. There should not necessarily be a fixed relationship between the feedback gains in both reflex limbs[43].

To our knowledge, there are no data regarding the relative strength of the gains in the three baroreflex effector limbs. It might well be that subjects with a low gain in the vagal limb have also low gains in the sympathetic limbs, amongst others, because part of the origin of these gains is to be found in the common afferent pathway of the reflex starting at the baroreceptors in the arterial wall up to and including the nucleus tractus solitarii in the brainstem. Inspection of the simulation results obtained under coupled gains (closed and open squares in *Figure 3* panel D) reveals that in such cases there is a seemingly linear relationship between BRS and blood pressure buffering capacity in healthy subjects as well as in patients.

Limitations of the model

Basic to our study is the representativeness of the mathematical model. The original model has extensively been validated[46], amongst others by comparing the results of modeled vagal blockade and of standing with real world observations. The modified model, however, has a simplified hemodynamic structure. Since the simulations addressed blood pressure and heart rate control in the supine posture only, the dynamic control capabilities of cardiac contractility and venous return on cardiac output and hence, blood pressure, have completely been removed (obviously, such a simplification cannot be made in cases where the average IBI changes due to an altering circulatory load). Elimination of these feedforward mechanisms enabled us to concentrate on the role of the various baroreflex gains, especially in the LF-band, rather than steady state phenomena in the lower frequencies. As our simulation results are still comparable with the various spectra produced by the original model, we do believe that our model still produces relevant spectra.

The modified model that was used for our current study generates and explains some situations that are known from the clinic. It is obvious that the resonance phenomenon in the LF band, generally known as Mayer waves[33], is strongly under influence of the baroreflex. The only situations in which Mayer waves hardly appear is when the sympathetic baroreflex gain to the peripheral resistance is small (see *Figure 2*, panel C2, dotted line). This simulation result parallels studies in rats[19], and in humans[42,45]. The relevance of the model is underscored by the observation that SBP variability in the LF band decreases for fixed interval (results not shown here). This phenomenon was described by Taylor and Eckberg[45] in a study in humans. The authors demonstrated that baroreflex mediated heart rate control was not effective in reducing blood pressure variability, that had a larger amplitude in sinus rhythm compared with fixed-interval atrial pacing.

Within the operating space — constituted by the ranges of the parameters as given in *Table 1*, in combination with baroreflex gain multiplier values between 0 and 3 — our model can be used without any difficulty. For example, as the baroreflex gain to the peripheral resistance (S_{PR}) should not have any influence on the transfer function, *Figure 2* panel C3 shows indeed that only varying S_{PR} produce almost the same transfer functions. The minimal differences between those functions can be explained by nonlinearities in the model. Further expansion of the operating space may therefore be not allowed. Furthermore, higher baroreflex gains would no longer be realistic and leads to, e.g., unacceptably high BPV values.

BRS can be enhanced by training[7] and the beneficial effects of a thus increased BRS have convincingly been demonstrated[27]. How this effect is accomplished remains uncertain. Inhibition of stressor induced heart rate increases may be one reason; the vagal feedback gain in the cardiac efferent limb may predominantly cause this effect. Inhibition of stressor induced blood pressure increases may be another reason; the sympathetic feedback gain in the baroreflex efferent limb to the peripheral vasculature may predominantly cause this effect. Both effects could help to inhibit a stressor induced raise of myocardial oxygen consumption, which is proportional to the product of heart rate and systolic blood pressure[3,29].

A final remark regards the phenomenon as seen in *Figure 2*, panel A3. It appears that BRS (the TF between 0.05 and 0.15 Hz.) may lower with high sympathetic gain to the heart. This is caused by the differences in the latencies/time constants in the sympathetic[17,41] and vagal[6,48] limbs, bringing the vagal and the sympathetic effects in counterphase in the BRS frequency band. Hence, there are situations thinkable in which cancellation of vagal effects on heart rate by concurring sympathetic effects on heart rate in counterphase incorrectly suggest a deficient baroreflex. For higher frequencies, the influence of the sympathetic feedback gain weakens and disappears due to a low pass filtering effect caused by slow neurotransmitter diffusion at the synaptic clefts[17].

CONCLUSIONS

In conclusion, our simulation study suggests that, within the limitations of the model, BRS and baroreflex mediated blood pressure buffering are unrelated baroreflex features unless there is a good physiological reason to assume a fixed relation between the baroreflex feedback gains in the efferent baroreflex limbs to the heart and peripheral vasculature.

Also, we conclude that baroreflex mediated blood pressure buffering capacity is almost uniquely determined by the sympathetic baroreflex feedback gain to the peripheral vasculature, while BRS is almost uniquely determined by the vagal feedback gain to the sinus node.

ACKNOWLEDGMENTS

This study was in part supported by the Netherlands Heart Foundation (grant 2003 B094). We thank prof. Karel H. Wesseling for critically reading this manuscript, and Sum-Che Man, MSc, for help in preparing the figures

REFERENCE LIST

1. Abrahamsson C, Ahlund C, Nordlander M, Lind L. A method for heart rate-corrected estimation of baroreflex sensitivity. *J Hypertens* 2003;21:2133–2140.
2. Aljuri N, Marini R, Cohen RJ. Test of dynamic closed-loop baroreflex and autoregulatory control of total peripheral resistance in intact and conscious sheep. *Am J Physiol Heart Circ Physiol* 2004;287:H2274–H2286.
3. Baller D, Bretschneider HJ, Hellige G. A critical look at currently used indirect indices of myocardial oxygen consumption. *Basic Res Cardiol* 1981;76:163–181.
4. Berger RD, Saul JP, Cohen RJ. Transfer function analysis of autonomic regulation I. Canine atrial rate response. *Am J Physiol* 1989;256:H142–H152.
5. Bertram D, Barres C, Cuisinaud G, Julien C. The arterial baroreceptor reflex of the rat exhibits positive feedback properties at the frequency of mayer waves. *J Physiol* 1998;513 (Pt 1):251–261.
6. Borst C, Karemaker JM. Time delays in the human baroreceptor reflex. *J Auton Nerv Syst* 1983;9:399–409.
7. Buch AN, Coote JH, Townend JN. Mortality, cardiac vagal control and physical training - what's the link? *Exp Physiol* 2002;87:423–435.
8. Burgess DE, Hundley JC, Li SG, Randall DC, Brown DR. First-order differential-delay equation for the baroreflex predicts the 0.4-Hz blood pressure rhythm in rats. *Am J Physiol* 1997;273:R1878–R1884.
9. Cevese A, Gulli G, Polati E, Gottin L, Grasso R. Baroreflex and oscillation of heart period at 0.1 Hz studied by alpha-blockade and cross-spectral analysis in healthy humans. *J Physiol* 2001;531:235–244.
10. Chapuis B, Vidal-Petiot E, Orea V, Barres C, Julien C. Linear modelling analysis of baroreflex control of arterial pressure variability in rats. *J Physiol* 2004;559:639–649.
11. Christou DD, Jones PP, Seals DR. Baroreflex buffering in sedentary and endurance exercise-trained healthy men. *Hypertension* 2003;41:1219–1222.
12. De Boer RW, Karemaker JM, Strackee J. Hemodynamic fluctuations and baroreflex sensitivity in humans: a beat-to-beat model. *Am J Physiol* 1987;253:H680–H689.
13. Eckberg DL. The human respiratory gate. *J Physiol* 2003;548.2:339–352.
14. Eckberg DL, Sleight P. Human baroreflexes in health and disease. 1992. *Clarendon Press, Oxford*.
15. Frederiks J, Swenne CA, TenVoorde BJ, Honzíková N, Levert JV, Maan AC et al. The importance of high-frequency paced breathing in spectral baroreflex sensitivity assessment. *J Hypertens* 2000;11:1635–1644.
16. Hammer PE, Saul JP. Resonance in a mathematical model of baroreflex control: arterial blood pressure waves accompanying postural stress. *Am J Physiol Regul Integr Comp Physiol* 2005;288:R1637–R1648.
17. Hill-Smith I, Purves RD. Synaptic delay in the heart: an inophoretic study. *J Physiol* (Lond) 1978;279:31–54.
18. Hyndman BW, Mohn RK. A model of the cardiac pacemaker and it's use in decoding the information content of cardiac intervals. *Automedica* 1973;1:239–252.
19. Japundzic N, Grichois ML, Zitoun P, Laude D, Elghozi JL. Spectral analysis of blood pressure and heart rate in conscious rats: effects of autonomic blockers. *J Auton Nerv Syst* 1990;30:91–100.
20. Jones PP, Christou DD, Jordan J, Seals DR. Baroreflex buffering is reduced with age in healthy men. *Circulation* 2003;107:1770–1774.
21. Jordan J, Tank J, Shannon JR, Diedrich A, Lipp A, Schroder C et al. Baroreflex buffering and susceptibility to vasoactive drugs. *Circulation* 2002;105:1459–1464.
22. Julien C. The enigma of Mayer waves: Facts and models. *Cardiovasc Res* 2006;70:12–21.
23. Just A, Wittmann U, Nafz B, Wagner CD, Ehmke H, Kirchheim HR et al. The blood pressure buffering capacity of nitric oxide by comparison to the baroreceptor reflex. *Am J Physiol* 1994;267:H521–H527.
24. Karemaker JM. Neurophysiology of the baroreceptor reflex. In: The beat-to-beat investigation of cardiovascular function. Kitney R, Rompelman O, eds. 1987. *Clarendon Press, Oxford*.
25. Katona PG, McLean M, Dighton DH, Guz A. Sympathetic and parasympathetic cardiac control in athletes and nonathletes at rest. *J Appl Physiol Respirat Environ Exercise Physiol* 1982;52:1652–1657.
26. Katona PG, Poitras JW, Barnett GO, Terry BS. Cardiac vagal efferent activity and heart period in the carotid sinus reflex. *Am J Physiol* 1970;218:1030–1037.
27. La Rovere MT, Bersano C, Gnemmi M, Specchia G, Schwartz PJ. Exercise-induced increase in baroreflex sensitivity predicts improved prognosis after myocardial infarction. *Circulation* 2002;106:945–949.
28. La Rovere MT, Bigger Jr JT, Marcus FI, Mortara A, Schwartz PJ. Baroreflex sensitivity and heart-rate variability in prediction of total cardiac mortality after myocardial infarction. *Lancet* 1998;351:478–484.
29. Laurent D, Bolene-Williams C, Williams FL, Katz LN. Effects of heart rate on coronary flow and cardiac oxygen consumption. *Am J Physiol* 1956;185:355–364.
30. Liu HK, Guild SJ, Ringwood JV, Barrett CJ, Leonard BL, Nguang SK et al. Dynamic baroreflex control of blood pressure: influence of the heart vs. peripheral resistance. *Am J Physiol Regul Integr Comp Physiol* 2002;283:R533–R542.
31. Madwed JB, Albrecht P, Mark RG, Cohen RJ. Low-frequency oscillations in arterial pressure and heart rate: a simple computer model. *Am J Physiol* 1989;256:H1573–H1579.
32. Malpas SC. Neural influences on cardiovascular variability: possibilities and pitfalls. *Am J Physiol Heart Circ Physiol* 2002;282:H6–20.
33. Mayer S. Studien zur Physiologie des Herzens und der Blutgefässe: V. Über spontane Blutdruckschwankungen. *Akad Wiss Math-Nat Kl* (Wien) 1876;74:281–307.
34. Parati G, Di Rienzo M, Mancia G. How to measure baroreflex sensitivity: from the cardiovascular laboratory to daily life. *J Hypertens* 2000;18:7–19.
35. Penáz J, Buriánek P. Zeitverlauf und Dynamik der durch Atmung ausgelösten Kreislaufänderungen beim Menschen. *Pflügers Arch* 1962;267:618–635.
36. Pickering TG, Gribbin B, Sleight P. Comparison of the reflex heart rate response to rising and falling arterial pressure in man. *Circ Res* 1972;6:277–283.
37. Pinna GD, Maestri R. Reliability of transfer function estimates in cardiovascular variability analysis. *Med Biol Eng Comput* 2001;39:338–347.
38. Pomeranz B, Macaulay RJ, Caudill MA, Kutz I, Adam D, Gordon D et al. Assessment of autonomic function in humans by heart rate spectral analysis. *Am J Physiol* 1985;248:H151–H153.
39. Robbe HWJ, Mulder LJM, Rüddel H, Langewitz WA, Veldman JBP, Mulder G. Assessment of baroreceptor reflex sensitivity by means of spectral analysis. *Hypertension* 1987;10:538–543.
40. Rosenblueth A, Simeone FA. The interrelations of vagal and accelerator effects on the cardiac rate. *Am J Physiol* 1934;110:42–45.
41. Saul JP, Berger RD, Albrecht P, Stein SP, Chen MH, Cohen RJ. Transfer function analysis of the circulation: unique insights into cardiovascular regulation. *Am J Physiol* 1991;261:H1231–H1245.
42. Scheffer GJ, TenVoorde BJ, Karemaker JM, Ros HH. Effects of epidural analgesia and atropine on heart rate and blood pressure variability: implications for the interpretation of beat-to-beat fluctuations. *Eur J Anaesthesiol* 1994;11:75–80.
43. Simms AE, Paton JF, Pickering AE. Disininhibition of the cardiac limb of the arterial baroreflex in rat: A role for metabotropic glutamate receptors in the nucleus tractus solitarii. *J Physiol* 2006.
44. Smyth HS, Sleight P, Pickering GW. Reflex regulation of arterial pressure during sleep in man: a quantitative method of assessing baroreflex sensitivity. *Circ Res* 1969;24:109–121.
45. Taylor JA, Eckberg DL. Fundamental relations between short-term RR interval and arterial pressure oscillations in humans. *Circulation* 1996;93:1527–1532.
46. Ten Voorde BJ, Kingma R. A baroreflex model of short term blood pressure and heart rate variability. *Stud Health Technol Inform* 2000;71:179–200.
47. Thrasher TN. Baroreceptors and the long-term control of blood pressure. *Exp Physiol* 2004;89:331–335.
48. Warner HR, Cox A. A mathematical model of heart rate control by sympathetic and vagus efferent information. *J Appl Physiol* 1962;17:349–355.
49. Wesseling KH, Settels JJ. Baromodulation explains short-term blood pressure variability. In: Psychophysiology of cardiovascular control. Orlebeke JF, Mulder G, VanDoornen LJP, eds. 1985. *Plenum Press, New York*.
50. Xavier-Neto J, Moreira E, Krieger E. Viscoelastic mechanisms of aortic baroreceptor resetting to hypotension and hypertension. *Am J Physiol* 1996;271:H1407–H1415.
51. Xie P, McDowell T, Chapleau M, Hajduczok G, Abboud F. Rapid baroreceptor resetting in chronic hypertension. Implications for normalization of arterial pressure. *Hypertension* 1991;17:72–79.